Water Practice & Technology

IWA PUBLISHING

Water Practice & Technology Vol 16 No 4, 1343 doi: 10.2166/wpt.2021.072

Phosphate removal by ion exchange in batch mode

T. E. Bektaş [a,*], B. Kıvanç Uğurluoğlu[b] and B. Tan[c]

[a] Department of Chemical Engineering, Faculty of Engineering, Çanakkale Onsekiz Mart University, 17100 Çanakkale, Turkey
[b] Department of Chemical Engineering, Faculty of Engineering and Architecture, Eskisehir Osmangazi University, 26480 Eskisehir, Turkey
[c] Department of Chemistry, Faculty of Sciences and Arts, Çanakkale Onsekiz Mart University, 17020 Çanakkale, Turkey
*Corresponding author. E-mail: ennilbektas@comu.edu.tr

TEB, 0000-0001-9180-3623

ABSTRACT

Water with phosphate concentrations above 2 μM may adversely affect aquatic life and human health. In this study, the parameters affecting phosphate removal from aqueous solutions by ion exchange were investigated – contact time and temperature, initial pH, initial phosphate concentration and resin dosage, and the presence of other ions. The best phosphate removal (99%) from 100 mg-P/L initial solution was observed at pH 10 and 25 °C after 3 hours of contact time. No negative phosphate removal results were obtained from phosphate solutions containing sulfate, nitrate and ammonium ions; i.e., resembling real wastewater. Desorption (with NaOH or NaCl) and recovery (with CaO) studies of phosphate sorbed by resin were also carried out, as well as thermodynamic investigations. The proportional desorbability of phosphate from the resin with NaCl was 85.6%. The recovery efficiency of phosphate was 79.4%. The sorption process was spontaneous and endothermic. The ion exchange mechanism was determined using different internal and external diffusion models. The mechanism controlling the removal of phosphate from aqueous solution is both internal and external diffusion. Application of the Langmuir and Freundlich isotherm models showed that the experimental results fit well with the Freundlich model.

Key words: ion exchange, isotherm, kinetic model, Lewatit Monoplus M 600, phosphate

HIGHLIGHTS

- The danger of phosphate in terms of water pollution.
- Selective and high phosphate removal using Lewatit MonoPlus M 600.
- Discussion of the mechanisms of phosphate removal.
- Desorption of phosphate with NaCl is easy.

INTRODUCTION

The most common types of phosphates present in natural water environments and wastewater are orthophosphates and polyphosphates. Phosphate pollution in wastewater is mostly caused by fertilization in agricultural areas, detergents, animal wastes and industrial activities. Phosphate in wastewater is one of the main factors that leads to the eutrophication and deterioration of water bodies, which leads to short and long-term environmental problems (Kilpimaaa *et al.* 2014). In such an environment, the depletion of oxygen content, color change, increased turbidity, excessive phosphate accumulation at the bottom, reduction in the number of species, decomposition and fouling are observed, and the environment gradually becomes unusable (Minareci *et al.* 2009).

In the WHO water criteria, the maximum phosphate concentration for first-class water quality in surface waters is 10 μg/L. The U.S. Environmental Protection Agency (USEPA) suggests that total P in streams or other flowing waters does not exceed 0.10 mg/L or 0.05 mg/L in any stream that reaches lakes or reservoirs (Polomski *et al.* 2009). Therefore, phosphate exceeding the recommended limit (10 μg/L) in water should be removed. Advanced treatment methods such as adsorption and ion exchange can be used. Various materials have been used as adsorbents, including fly ash (63.2 mg/g) (Lu *et al.* 2009), red-mud (113.87 mg/g) (Li *et al.* 2006), alunite (118 mg/g) (Özacar 2003), La(III)-bentonite/chitosan composite (23.52 mg/g) (Xu *et al.* 2020), modified biochar (265.5 mg/g) (Nakarmi *et al.* 2020), crab shell (108.9 mg/g) (Jeon & Yeom 2009), egg shell

(23 mg/g) (Köse & Kıvanç 2011), anion exchanger (16 mg P-PO_4/g) (Bui *et al.* 2021) and ion exchange fiber (16.2 mg/g) (Blaney *et al.* 2007).

In water treatment applications, ion exchange involves the replacement of an ion in the aqueous phase with an ion from the resin phase. The ion exchanger is insoluble in water and can be a substance of natural origin such as zeolite or kaolinite, or a synthetic substance such as a polymer. These materials have fixed-charged functional groups on their internal and/or external surfaces, and the opposite charged (counter-) ions attached to these groups are found. If the functional group is negative, the counter-ion attached is a cation. If it is positive, the counter-ion is an anion and can exchange with another counter-ion in the aqueous phase. For most ion exchange applications in water treatment, synthetic organic resins are utilized because of their relatively large available exchange capacities and ease of regeneration (Helfferich 1962).

The aim of this work was to investigate the phosphate removal ability of Lewatit Monoplus M 600 anion exchange resin from aqueous solution in batch mode operation. Various sorption kinetic models for phosphate were investigated. Along with the sorption process, the effects of contact time and temperature, initial solution pH, and initial phosphate concentration and resin dosage, and the presence of other ions on phosphate removal efficiency were investigated. Isotherm studies were also done and the thermodynamic parameters for phosphate removal determined.

EXPERIMENTAL

Materials

Lewatit MonoPlus M 600 was a strongly basic, gelular anion exchange resin with beads of uniform size based on a styrene-divinylbenzene copolymer. It was kindly supplied by Ökotek Chem., Turkey. The resin's characteristics are given in Table 1. A stock phosphate solution was prepared by dissolving anhydrous potassium dihydrogen phosphate (KH_2PO_4) in distilled water to give a concentration of 5,000 mg-PO_4^{3-}/L. This was diluted when necessary.

Table 1 | Properties of Lewatit MonoPlus M 600

Functional group	Quaternary amine, type II
Structure	Gel type beads
Mean bead size (mm)	0.6 ($\pm$0.05)
Bulk density (g/L)	700
Density approximately (g/mL)	1.1
Maximum operating temperature (°C)	30
Total capacity (min. solution/L resin)	1.25
pH range	0–11

Batch sorption of phosphate

In all experiments except the dosage study, a fixed amount of resin was contacted with 50 mL of 100 mg/L phosphate solution, in a capped flask shaken at 140 rpm in a water bath with a temperature-controlled shaker (Memmert). After the samples were filtered, the supernatant solution was analyzed in a spectrophotometer (Hach DR-2000) using the molybdovanadat method to determine the phosphate concentration (Köse & Kıvanç 2011).

For the kinetic tests, samples were taken from the shaker water bath at fixed time intervals at 25, 35 and 45 °C, and filtered, and the supernatant solution phosphate concentration determined. In order to see the effect of pH, the solution's initial pH was adjusted between 2 and 10.

For the sorption isotherm study and to investigate the effect of initial concentration on phosphate removal, solutions of different phosphate concentrations were contacted with different resin amounts for 3 hours at 25 °C and the optimum pH.

The effect of ions such as sulphate, nitrate and ammonium, which are present with the phosphate ions in real wastewaters, on phosphate removal was investigated. K_2SO_4, $NaNO_3$ and NH_4Cl were used to obtain the respective anions. Tests were carried out at 100 mg-PO_4^{3-}/L, with 10 or 50 mg/L concentrations of each ion.

At the end of the sorption process performed at optimum values, the resin was separated from the solution by centrifugation and filtration, and shaken with 50 mL of 0.5 M NaOH or NaCl solution for 2 hours. The concentration of phosphate ions desorbed from the resin was determined. 4.4 mg of solid CaO was added to the desorption solution to recover the desorbed phosphate.

The amount of phosphate adsorbed, q (mg/g), was calculated using the following equation:

$$q = \frac{(C_o - C_e)V}{m} \tag{1}$$

The percentage of phosphate removed (%) from solution was calculated using the equation:

$$\%\,\text{Removal} = \frac{(C_o - C_e)}{C_o} \times 100 \tag{2}$$

where C_o and C_e are the initial and equilibrium phosphate concentrations (mg/L) respectively, m is the mass of resin (g), and V is the volume of the solution (L).

RESULTS AND DISCUSSION

Effect of contact time and temperature, and kinetic models of ion exchange

The sorption of phosphate on resin was observed as a function of contact time to determine the equilibrium time at 25, 35 and 45 °C. From Figure 1, the percent removal of phosphate increased with increase in contact time. Phosphate removal was rapid initially then increased slowly until saturation. In the early stages, the increase in the phosphate concentration gradient between the solution and the resin increased the sorption rate. In addition, there were many vacant sites initially in the resin phase. Since there was no significant change in the phosphate concentration in the equilibrium, the percentage of phosphate removal remained constant. Equilibrium was attained within 3 hours for all temperatures.

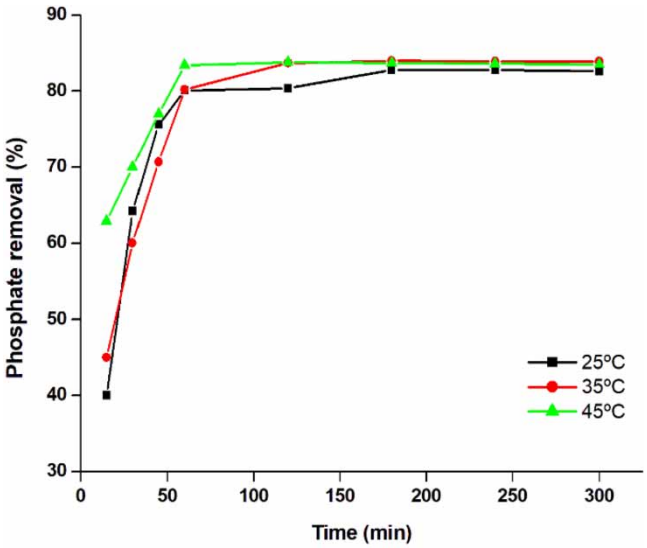

Figure 1 | Effect of contact time and temperature on phosphate removal onto resin.

The effect of temperature on phosphate sorption was investigated by varying the temperature from 25 to 45 °C. Thermodynamically, the changes in standard free energy ($\Delta G°$), enthalpy ($\Delta H°$) and entropy ($\Delta S°$) of sorption were calculated using Equations (3)–(5). The values obtained are summarized in Table 2.

$$\Delta G^\circ = -\text{RTlnK} \tag{3}$$

Table 2 | Thermodynamic parameters for phosphate sorption onto resin

T(°C)	K	ΔG° (kJ/mol)	ΔH° (kJ/mol)	ΔS° (j/mol K)
25	4.81	−3.89	2.57	0.022
35	5.17	−4.20		
45	5.13	−4.32		

where R is the gas constant, K is the equilibrium constant and T is the temperature in K. The equilibrium constant (K) is calculated according to Equation (4):

$$K = \frac{C_s}{C_e} \tag{4}$$

where C_s is the equilibrium concentration of phosphate on resin (mg/g), C_e is the equilibrium concentration of phosphate in solution (mg/L). According to the van't Hoff equation:

$$\ln K = \frac{\Delta S^\circ}{R} - \frac{\Delta H^\circ}{RT} \tag{5}$$

Figure 2 gives the linear graph of lnK versus 1/T. The line's slope gives $\Delta H°$ (kJ/mol) and the intercept on the x-axis gives $\Delta S°$ (J/mol K). Negative $\Delta G°$ values at different temperatures showed that the sorption process was spontaneous. Sorption is endothermic if ΔH° is positive, and a positive $\Delta S°$ value indicates increasing irregularity during sorption.

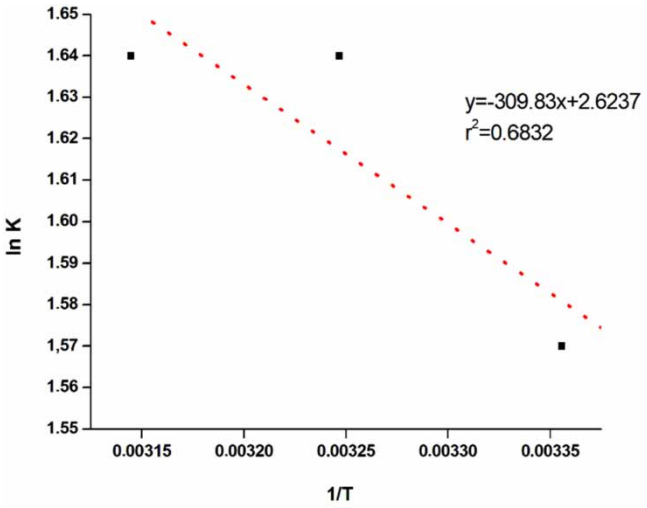

Figure 2 | Van't Hoff plot for phosphate sorption onto resin.

Determining the mass transfer parameters to explain the mechanism of the sorption process is important for process design. Mass transfer kinetics for the sorption process includes three steps. The first step is the external diffusion of the adsorbate in the liquid phase, which is transferred through the liquid film around the resin or adsorbent. The difference in concentration between the bulk solution and the surface of the adsorbent is the driving force of the external diffusion. The second step is the internal diffusion of the adsorbate, which is transferred to the pores and channels of the resin or adsorbent. The third step is binding of the adsorbate to the active sites of the resin or adsorbent. The slowest of these steps controls the sorption process and is the rate-limiting step. The prediction of the rate-limiting step is very important for the design of a sorption process. It's assumed that the third step is rapid when compared to the first two steps. Therefore, there are two main mass transfer mechanisms in a sorption process, internal and external diffusion (Figure 3). In order to explain the mechanism involved in the

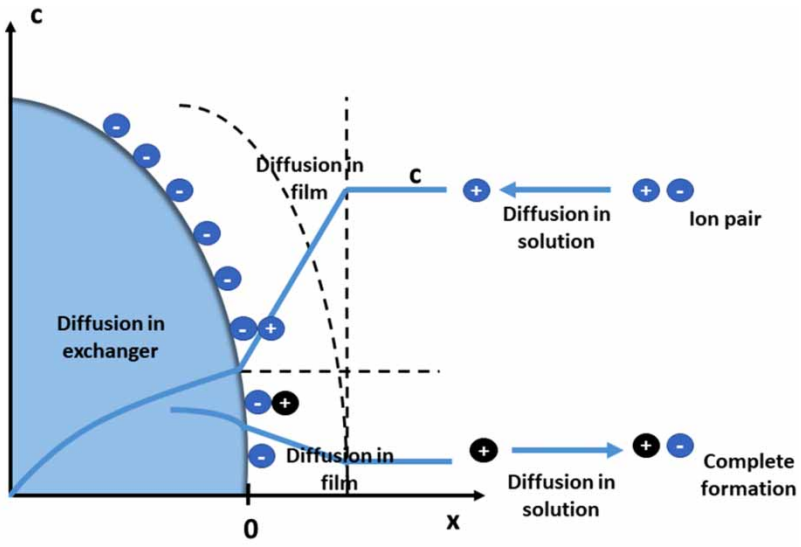

Figure 3 | Ion exchange mechanism.

ion exchange process, several diffusion models were used in this study (Al-Duri & McKay 1988; McKay & Al-Duri 1990; Ho *et al.* 2000; Ko *et al.* 2002; Choong *et al.* 2006; Girish & Murty 2016; Yao & Chen 2017; Wang & Guo 2020).

Boyd's diffusion equations

Boyd's external model has been applied to describe the diffusion of adsorbate through a bounding liquid film (Boyd *et al.* 1947):

$$-\ln\left(1-\frac{q_t}{q_e}\right)=k_b t \tag{6}$$

$$F=\frac{q_t}{q_e} \tag{7}$$

where q_t and q_e are the amounts of phosphate sorbed (mg/g) at any time t and equilibrium time (min), respectively, and k_b is the Boyd constant (min^{-1}).

Boyd *et al.* (1947) represented an internal diffusion model as follows:

$$F=1-\frac{6}{\pi^2}\sum_{z=1}^{\infty}\frac{1}{z^2}e^{-z^2Bt} \tag{8}$$

$$B \text{ is a parameter defined as: } B=\frac{\pi^2 D_{\text{eff}}}{r^2} \tag{9}$$

where r is the radius of the resin particle (cm), D_{eff} is the effective intraparticle diffusion coefficient of adsorbate in the adsorbent phase (cm^2/min), and z is an integer.

For values of F ranging from 0 to 0.85:

$$Bt=2\pi-\frac{\pi^2 F}{3}-2\pi\left(1-\frac{\pi F}{3}\right)^{1/2} \tag{10}$$

while for values ranging from 0.86 to 1:

$$Bt=-\ln\frac{\pi^2}{6}(1-F) \tag{11}$$

The plots for diffusion coefficient determination are shown in Figure 4(a) and 4(b) with the linear fitting equations and regression coefficients (R^2 values). The Boyd constant (k_b) was calculated from the slope of the plot of $-\ln(1 - F)$ versus time (Figure 4(a)). Figure 4(b) showed that experimental data were plotted according to Boyd's internal diffusion model. If the plot of Bt versus t passed through its origin, it could be said that the mechanism controlling the sorption process is internal diffusion (Yakub *et al.* 2019; Wang & Guo 2020). Therefore, Figure 4 shows that external diffusion was as important as internal diffusion for the sorption mechanism of phosphate onto ion exchange resin. According to Table 3, R^2 values for both Boyd's diffusion models at different temperatures vary between 0.88 and 1. The magnitude of D_{eff} is 10^{-5}–10^{-12} cm^2/s sorption type can be explained by chemisorption (Girish & Ramachandra 2016). Apart from the correlation coefficient (R^2), the chi-square (X^2) test was used to measure the goodness-of fit. The chi-square test defined by Equation (12) (Das *et al.* 2021):

$$X^2 = \sum \frac{(q_{exp} - q_{cal})^2}{q_{cal}} \tag{12}$$

where q_{exp} and q_{cal} are the experimental and calculated values, respectively. Smaller chi-square values indicate better curve fitting.

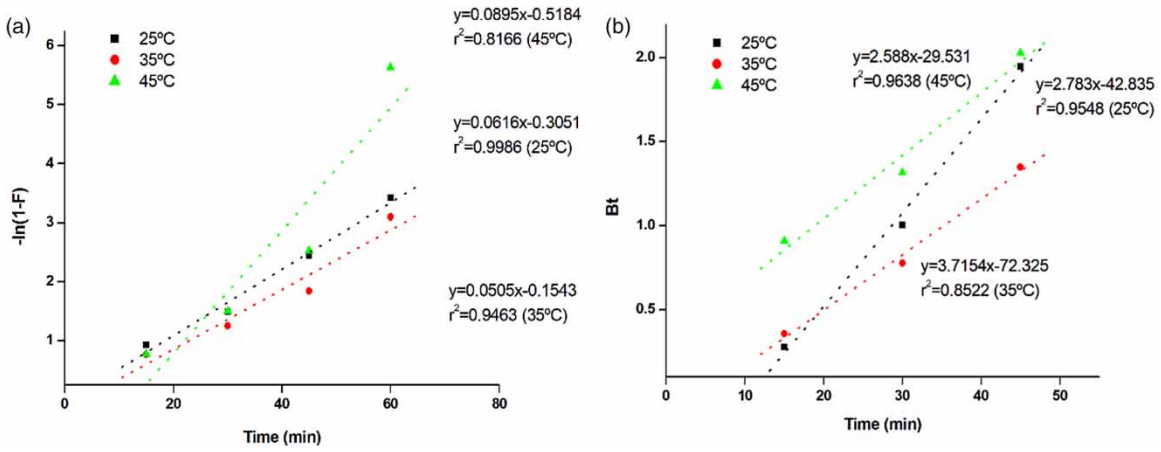

Figure 4 | Boyd model (a) external diffusion (b) internal diffusion for phosphate removal onto resin.

Table 3 | Different diffusion model parameters for phosphate sorption on resin

Kinetic models	Parameters	25 °C	35 °C	45 °C
Boyd's External Diffusion Model	$k_b(min^{-1})$	0.056	0.0505	0.104
	R^2	0.98	0.95	0.88
	X^2	0.033	0.066	0.99
Boyd's Internal Diffusion Model	$D_{eff}(cm^2/s)$	1.5×10^{-6}	5.02×10^{-8}	8.45×10^{-8}
	R^2	1	0.99	0.98
	X^2	0	0.13	0.59
Frusawa and Smith External Diffusion Model	$\beta_L(m/s)$	0.016	0.017	0.02
	R^2	0.98	0.99	0.99
	X^2	3.07	1.18	0.67
Weber-Morris Internal Diffusion Model	$k_i(mg/g\ min^{1/2})$	0.799	0.906	1.003
	D_{id} (cm/min)	1.17×10^{-5}	1.467×10^{-5}	1.8×10^{-5}
	R^2	0.98	0.99	0.98
	X^2	0.01	0.0002	0.02

Frusawa and Smith external diffusion model

The Furusawa and Smith model was used to analyse the effect of external mass transfer resistance on sorption rate. This model is expressed by Equation (13) (Fu *et al.* 2012; Girish & Murty 2016; Yakubu & Owabor

2018; Yakub *et al.* 2019)

$$\ln\left(\frac{C_t}{C_o} - \frac{1}{1+mK_L}\right) = \ln\frac{mK_L}{1+mK_L} - \frac{1+mK_L}{mK_L}\beta_L S_S t \tag{13}$$

where C_t is the concentration at time t (mg/L), C_0 is the initial phosphate concentration (mg/L), m is the adsorbent mass per unit volume of the phosphate solution (g/L), K_L is the Langmuir constant (obtained by multiplying Qo and b) (L/mg), β_L is the mass transfer coefficient (m/s) and Ss is the outer surface of the adsorbent per unit volume of phosphate solution (m^{-1}). A linear plot of $Y(t) = \ln(C_t/C_o - 1/1 + mK_L)$ versus time was used to find the coefficient β_L (Figure 5). External mass transfer resistance is generally related to the mass transfer coefficient, and increasing this coefficient decreases the resistance. As can be seen from Table 3, the mass transfer coefficients are large and the external mass transfer rate is accordingly high for all temperatures.

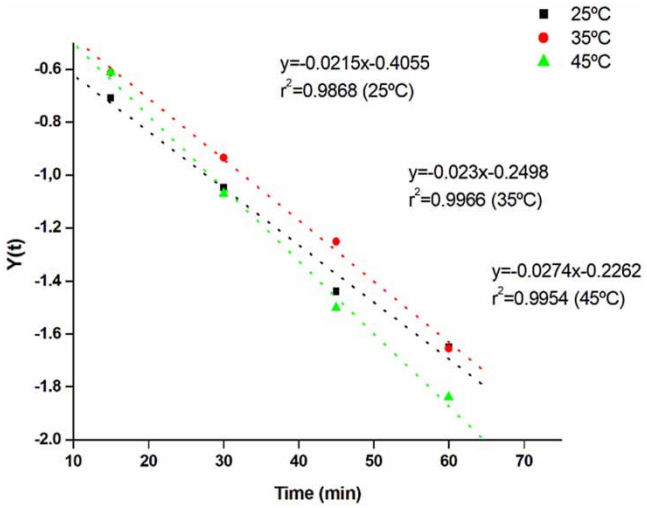

Figure 5 | Frusawa and Smith external diffusion model.

Weber-Morris internal diffusion model

If the rate-limiting step in the sorption process is intraparticle diffusion, the Weber-Morris diffusion model is often used. It is represented by Equation (14) (Ho *et al.* 2000; Yakout & Elsherif 2010; Velempini *et al.* 2017; Jia *et al.* 2020)

$$q_t = k_i t^{1/2} + C \tag{14}$$

where C *(mg/g)* is a parameter that indicates the boundary layer effects and k_i is the intraparticle diffusion rate constant (mg/g $min^{1/2}$), and is related to the intraparticle diffusivity D_{id} (cm/min) as described by Equation (15) (Teixeira *et al.* 2013).

$$k_i = \left(\frac{3q_e}{d_p}\right)\sqrt{\frac{D_{id}}{\pi}} \tag{15}$$

where d_p is the particle diameter (cm) and q_e is the equilibrium sorption capacity (mg/g). k_i and C can both be determined from the slope and intercept of Figure 6.

If intraparticle diffusion is involved in the sorption process, a plot of q_t versus $t^{1/2}$ would be a good linear relationship and pass through the origin (Poots *et al.* 1976). As seen from Figure 5, deviation of the line from the origin indicates that the rate limiting step is not only intraparticle diffusion. This implies that phosphate sorption was a multistage process. Figure 6 had two linear parts. The initial part represents external diffusion and the second intraparticle diffusion. The parameters of intraparticle diffusion are shown in Table 3. The value of

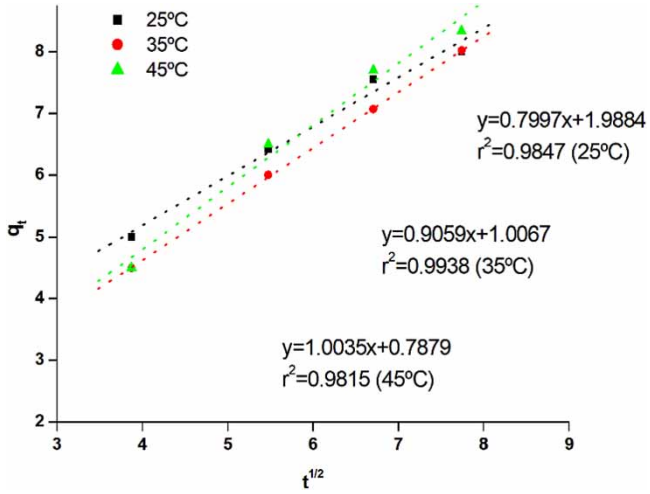

Figure 6 | Weber-Morris internal diffusion model.

$R^2 > 0.98$ in this model justifies the mechanism for the diffusion of phosphate. The experimental and calculated quantities sorbed at equilibrium (q_{eexp} and q_{ecal}) from the model agreed closely given the low values for the chi square test (X^2).

Effect of initial pH

The effect of pH on phosphate sorption is shown in Figure 7. At pH 2, the sorption percentage of phosphate onto resin was 80%. At pH 10, the phosphate sorption percentage was 99%, the highest achieved. At low pH values, phosphate exists predominantly as H_3PO_4, which is neutral and has difficulty entering resin pores because of its relatively large size. With increasing pH values, the major phosphate species are H_2PO^{4-}, HPO_4^{2-} and PO_4^{3-}, which can sorb onto the resin (Ruixia *et al.* 2002; Taleb *et al.* 2008).

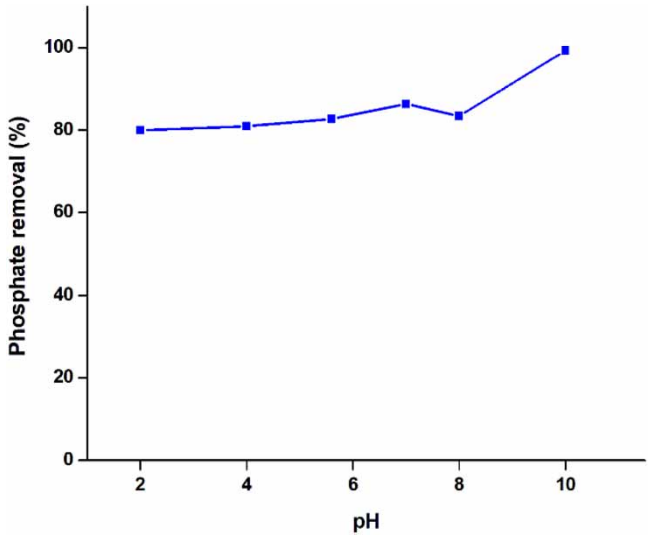

Figure 7 | Effect of initial pH on phosphate removal onto resin.

Effect of initial phosphate concentration and resin dosage

Phosphate sorption onto the resin was investigated as a function of resin dosage (between 0.1 and 1 g/50 mL) at five different initial phosphate concentrations (between 50 and 200 mg/L). The resin's removal efficiency varied approximately from 71 to 99.8% with increasing resin concentration, for all initial phosphate concentrations (Figure 8). Proportional phosphate removal increased with increasing resin dosage due to the increasing sorption surface area.

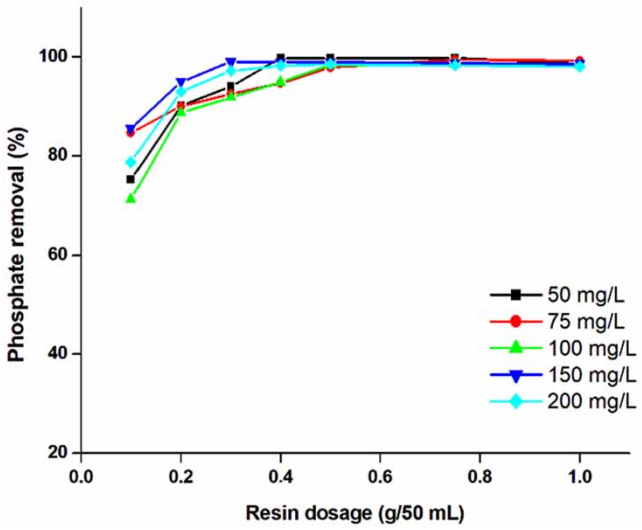

Figure 8 | Effect of initial phosphate concentration and resin dosage on phosphate removal by ion exchange.

The experimental data were applied to the Langmuir and Freundlich isotherm models. The linear forms of the isotherm equations are given by Equations (16) and (17) (Weber 1972):

$$\frac{C_e}{q_e} = \frac{1}{Q_o b} + \frac{C_e}{Q_o} \tag{16}$$

$$\log q_e = \log K + \frac{1}{n}\log C_e \tag{17}$$

where C_e is the equilibrium concentration (mg/L), q_e is the amount of phosphate sorbed at equilibrium (mg/g), and Q_o and b are the Langmuir constants related to sorption capacity and energy of sorption, respectively. Also, K and n are the Freundlich constants, being indicative of the sorption capacity and intensity of sorption, respectively. The isotherm model constants are given in Table 4 and a graph of the linear Freundlich equation is shown in Figure 9. According to the correlation coefficients, the Freundlich equation fits the experimental data better than the Langmuir equation, signifying heterogeneous surface binding.

Table 4 | Langmuir and Freundlich constants for phosphate sorption on resin

Langmuir isotherm			Freundlich isotherm		
Q_o (mg PO_4^{3-}/g)	b (L/mg)	R^2	K (mg/g)	n	R^2
29.07	0.5	0.84	9.27	1.77	0.94

Effect of other ions

The parameters affecting phosphate removal by the resin were investigated for the aqueous solution. However, there are other ions besides the phosphate anion in real wastewaters. Sulphate, nitrate and ammonium ions were used as foreign ions, and the effects of their presence on phosphate removal studied. The experimental data are shown in Figure 10, which shows that, from solutions of 10 or 50 mg/L of sulfate, nitrate and ammonium ions coexisting with 100 mg-phosphate/L, phosphate removal did not change significantly.

Desorption and recovery studies

Desorption and recovery processes are important in terms of resin reusability and cost. The experiments were conducted for contact time of 3 hours using 0.5 g-resin/50 mL and 100 mg-P/L at pH 10. After three hours sorption, the phosphate-loaded resin was filtered from the aqueous solution. The desorption experiments were carried out in 0.5 M NaOH and 0.5 M NaCl solutions, in batch mode, to recover the phosphate from the resin.

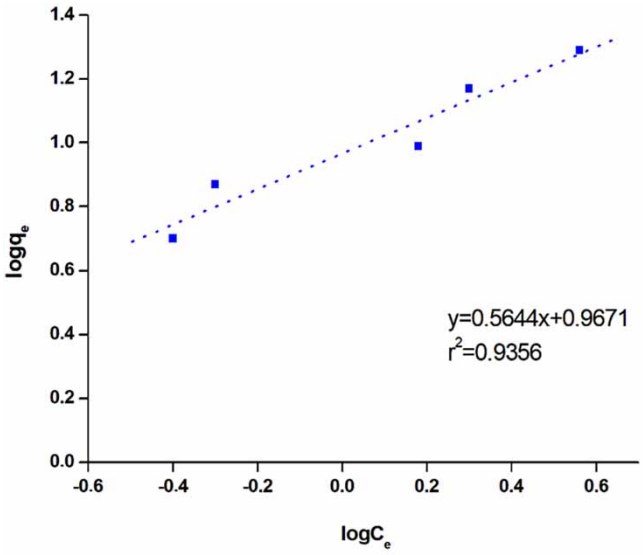

Figure 9 | Freundlich isotherm plots for phosphate sorption.

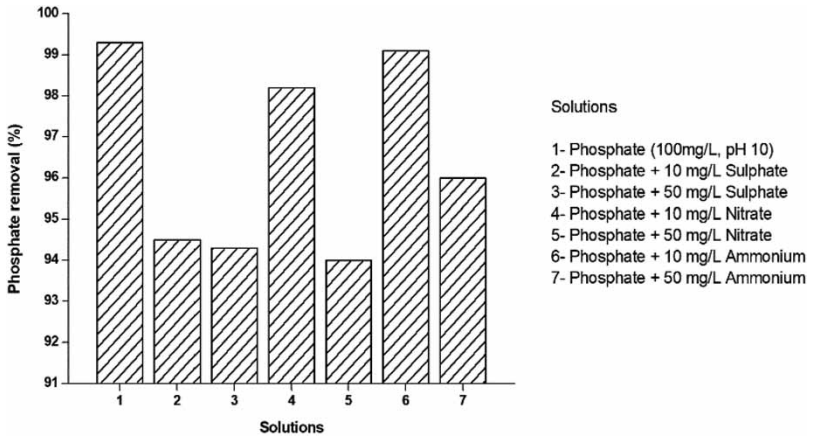

Figure 10 | Effect of other ions on phosphate sorption.

Proportional desorption was calculated using Equation (18):

$$\text{Desorbability}(\%) = \frac{\text{Amount of desorbed to the elution medium}}{\text{Amount of ion sorbed on the adsorbent}} \times 100 \quad (18)$$

The proportional desorbability of phosphate was determined as 70.5 and 85.6% with NaOH and NaCl, respectively. Solid calcium oxide was added to the NaCl solution to recover the desorbed phosphate as calcium phosphate, giving a yield of 79.4%.

CONCLUSION

Use of Lewatit Monoplus M600 anion exchange resin for phosphate removal from aqueous solutions was investigated The amount of phosphate sorbed from aqueous solution increased with contact time, equilibrium being achieved within 180 min. No significant temperature effect on phosphate removal was observed. The optimum resin dose for phosphate removal was 0.5 g/50 mL. The values of $\Delta G°$ and $\Delta H°$ show that phosphate sorption on the resin is spontaneous and endothermic. The kinetic results show that external and internal diffusion are equally important for phosphate sorption onto the resin. The Freundlich isotherm model showed the best fit for the experimental results. Resin removal efficiency was high (99%) at initial pH 10. The presence of foreign

ions had no significant effect on phosphate removal. The desorption study showed that phosphate is desorbed easily with NaCl. Precipitate recovered in the form of calcium phosphate can be used as fertilizer or soil conditioner.

AUTHOR CONTRIBUTION STATEMENT

T.E.Bektaş: design and conduct of experiments, creation of the article. B. Kıvanç Uğurluoğlu: experimental work, B.Tan: editing. All authors discussed the results and contributed to the final manuscript.

DATA AVAILABILITY STATEMENT

All relevant data are included in the paper or its Supplementary Information.

REFERENCES

Al-Duri, B. & McKay, G. 1988 Basic dye adsorption on carbon using a solid-phase diffusion model. *The Chemical Engineering Journal* **38**, 23–31. https://doi.org/10.1016/0300-9467(88)80050-9.

Blaney, L. M., Cinar, S. & SenGupta, A. K. 2007 Hybrid anion exchanger for trace phosphate removal from water and wastewater. *Water Research* **4**, 1603–1613. https://doi.org/10.1016/j.watres.2007.01.008.

Boyd, G. E., Adamson, A. W. & Myers, L. S. 1947 The exchange adsorption of ions from aqueous solutions by organic zeolites, II kinetics. *Journal of the American Chemical Society* **69**, 2836–2848. https://doi.org/10.1021/ja01203a066.

Bui, T. H., Hong, S. P., Kim, C. & Yoon, J. 2021 Performance analysis of hydrated Zr(IV) oxide nanoparticle-impregnated anion exchange resin for selective phosphate removal. *Journal of Colloid and Interface Science* **586**, 741–747. https://doi.org/10.1016/j.jcis.2020.10.143.

Choong, T. S. Y., Wong, T. N., Chuah, T. G. & Idris, A. 2006 Film-pore-concentration dependent surface diffusion model for the adsorption of dye onto palm kernel shell activated carbon. *Journal of Colloid and Interface Science* **301**, 436–440. doi:10.1016/j.jcis.2006.05.033.

Das, P., Nisa, S., Debnath, A. & Saha, B. 2021 Enhanced adsorptive removal of toxic anionic dye by novel magnetic polymeric nanocomposite:optimization of process parameters. *Journal of Dispersion Science and Technology*. https://doi.org/10.1080/01932691.2020.1845958.

Fu, D., Zhang, Y., Lv, F., Chu, P. K. & Shang, J. 2012 Removal of organic materials from TNT red water by Bamboo Charcoal adsorption. *Chemical Engineering Journal* **193–194**, 39–49. https://doi.org/10.1016/j.cej.2012.03.039.

Girish, C. R. & Murty, V. R. 2016 Mass transfer studies on adsorption of phenol from wastewater using lantana camara, forest waste. *International Journal of Chemical Engineering*, 5809505. https://doi.org/10.1155/2016/5809505.

Girish, C. & Ramachandra, V. M. 2016 Mass transfer studies on adsorption of phenol from wastewater using *Lantana camara*, forest waste. *International Journal of Chemical Engineering* **6**(2), 11. https://doi.org/10.1155/2016/5809505.

Helfferich, F. 1962 *Ion Exchange*. McGraw-Hill, New York. https://doi.org/10.1126/science.138.3537.133.

Ho, Y. S., Ng, J. C. Y. & McKay, G. 2000 Kinetics of pollutant sorption by biosorbents. Review. *Separation and Purification Methods* **29**(2), 189–232.

Jeon, D. J. & Yeom, S. H. 2009 Recycling wasted biomaterial, crab shells, as an adsorbent for the removal of high concentration of phosphate. *Bioresource Technology* **100**, 2646–2649. doi:10.1016/j.biortech.2008.11.035.

Jia, Z., Zeng, W., Xu, H., Li, S. & Peng, Y. 2020 Adsorption removal and reuse of phosphate from wastewater using a novel adsorbent of lanthanum-modified platanus biochar. *Process Safety and Environmental Protection* **140**, 221–232. https://doi.org/10.1016/j.psep.2020.05.017.

Kilpimaaa, S., Runttia, H., Kangasa, T., Lassia, U. & Kuokkanen, T. 2014 Removal of phosphate and nitrate over a modified carbon residue from biomass gasification. *Chemical Engineering Research and Design* **92**, 1923–1933. https://doi.org/10.1016/j.cherd.2014.03.019.

Ko, D. C. K., Porter, J. F. & McKay, G. 2002 A branched pore model analysis for the adsorption of acid dyes on activated carbon. *Adsorption* **8**, 171–188. https://doi.org/10.1023/A:1021283731952.

Köse, T. E. & Kıvanç, B. 2011 Adsorption of phosphate from aqueous solutions using calcined waste eggshell. *Chemical Engineering Journal* **178**, 34–39. https://doi.org/10.1016/j.cej.2011.09.129.

Li, Y., Liu, C., Luan, Z., Peng, X., Zu, C., Chen, Z., Zhang, Z., Fan, J. & Jia, Z. 2006 Phosphate removal from aqueous solutions raw and activated red mud and fly ash. *Journal of Hazardous Materials B.* **137**, 374–383. https://doi.org/10.1016/j.jhazmat.2006.02.011.

Lu, S. G., Bai, S. Q. & Shan, H. D. 2009 Removal mechanism of phosphate from aqueous solution by fly ash. *Journal of Hazardous Materials* **161**, 95–101. https://doi.org/10.1016/j.jhazmat.2008.02.123.

McKay, G. & Al-Duri, B. 1990 Study of the mechanism of pore diffusion in batch adsorption systems. *Journal of Chemical Technology & Biotechnology* **48**, 269–285. https://doi.org/10.1002/jctb.280480304.

Minareci, O., Minareci, E. & Öztürk, M. 2009 Investigation of detergent, phosphate and boron pollution in Karaçay (Manisa). *Ege University Journal of Fisheries & Aquatic Sciences* **26**(3), 171–177. https://doi.org/10.12714/egejfas.2009.26.3.5000156541.

Nakarmi, A., Bourdo, S. E., Ruhl, L., Kanel, S., Nadagouda, M., Alla, P. K., Pavel, I. & Viswanathan, T. 2020 Benign zinc oxide betaine-modified biochar nanocomposites for phosphate removal from aqueous solutions. *Journal of Environmental Management* **272**, 111048. https://doi.org/10.1016/j.jenvman.2020.111048.

Özacar, M. 2003 Equilibrium and kinetic modeling of adsorption of phosphorus on calcined alunite. *Adsorption* **9**, 125–132. https://doi.org/10.1023/A:1024289209583.

Polomski, R. F., Taylor, M. D., Bielenberg, D. G., Bridges, W. C., Klaine, S. J. & Whitwell, T. 2009 Nitrogen and phosphorus remediation by three floating aquatic macrophytes in greenhouse-based laboratory-scale subsurface constructed wetlands. *Water, Air, and Soil Pollution* **197**, 223–232. doi:10.1007/s11270-008-9805-x.

Poots, V. J. P., McKay, G. & Healy, J. J. 1976 The removal of acid dye from effluent using natural adsorbents – II Wood. *Water Resources* **10**, 1067–1070. https://doi.org/10.1016/0043-1354(76)90037-3.

Ruixia, L., Jinlong, G. & Hongxiao, T. 2002 Adsorption of fluoride, phosphate and arsenate ions on a new type of ion exchange fiber. *Journal of Colloid and Interface Science* **248**, 268–274. https://doi.org/10.1006/jcis.2002.8260.

Taleb, M. F., Mahmoud, G. A., Elsigeny, S. M. & Hegazy, E. A. 2008 Adsorption and desorption of phosphate and nitrate ions quaternary (polypropylene-g-N,N-dimethylamino ethylmethacrylate) graft copolymer. *Journal of Hazardous Materials* **159**, 372–379. https://doi.org/10.1016/j.jhazmat.2008.02.028.

Teixeira, R. N. P., Neto, V. D. S., Oliveira, J. T., Oliveira, T. C., Melo, D. Q., Silva, M. A. A. & Nascimento, R. F. 2013 Study on the use of roasted barley powder for adsorption of Cu^{2+} ions in batch experiments and in fixed bed columns. *Bioresources* **8**(3), 3556–3573. https://doi.org/10.15376/biores.8.3.3556-3573.

Velempini, T., Pillay, K. & Mbianda, X. Y. 2017 Kinetic and thermodynamic studies for the removal of Cr(VI) from aqueous solutions using phosphonic acid functionalized multiwalled carbon nanotubes. *Research Journal of Environmental Sciences* **11**(3), 116–129. https://doi.org/10.3923/rjes.2017.116.129.

Wang, J. & Guo, X. 2020 Adsorption kinetic models: physical meanings, applications, and solving methods. *Journal of Hazardous Material* **390**, 122156. https://doi.org/10.1016/j.jhazmat.2020.122156.

Weber, W. J. 1972 *Physicochemical Processes for Water Quality Control*. Wiley, New York, p. 640. https://doi.org/10.1002/aic.690190245.

Xu, X., Cheng, Y., Wu, X., Fan, P. & Song, R. 2020 La(III)-bentonite/chitosan composite, A new type adsorbent for rapid removal of phosphate from water bodies. *Applied Clay Science* **190**, 105547. https://doi.org/10.1016/j.clay.2020.105547.

Yakout, S. M. & Elsherif, E. 2010 Batch kinetics, isotherm and thermodynamic studies of adsorption of strontium from aqueous solutions onto low cost rice-straw based carbons. *Carbon-Science and Technology* **1**, 144–153.

Yakub, E., Agarry, S. E., Omoruwou, F. & Owabor, C. N. 2019 Comparative study of the batch adsorption kinetics and mass transfer in phenol-sand and phenol-clay adsorption systems. *Particulate Science and Technology* **38**(7), 801–811. https://doi.org/10.1080/02726351.2019.1616862.

Yakubu, E. E. & Owabor, C. 2018 The effect of mass transfer resistance on the adsorption rate of phenol in soil sediments. *American Journal of Environmental Science and Engineering* **2**(4), 56–64. https://doi.org/10.1080/02726351.2019.1616862.

Yao, C. & Chen, T. 2017 A film-diffusion-based adsorption kinetic equation and its application. *Chemical Engineering Research and Design* **119**, 87–92. https://doi.org/10.1016/j.cherd.2017.01.004.

First received 9 March 2021; accepted in revised form 21 July 2021. Available online 4 August 2021